

See discussions, stats, and author profiles for this publication at: <https://www.researchgate.net/publication/281140887>

Like-Charge Guanidinium Pairing between Ligand and Receptor: An Unusual Interaction for Drug Discovery and Design?

ARTICLE in THE JOURNAL OF PHYSICAL CHEMISTRY B · AUGUST 2015

Impact Factor: 3.3 · DOI: 10.1021/acs.jpcb.5b04130 · Source: PubMed

READS

43

11 AUTHORS, INCLUDING:



Zhijian Xu

Shanghai Institute of Materia Medica, Chinese ...

31 PUBLICATIONS 245 CITATIONS

SEE PROFILE



Yingtao Liu

Shanghai Institute of Materia and Medica, Chi...

25 PUBLICATIONS 402 CITATIONS

SEE PROFILE



Jiye Shi

Union Chimique Belge (UCB)

80 PUBLICATIONS 1,889 CITATIONS

SEE PROFILE



Weiliang Zhu

Shanghai Institute of Materia Medica

209 PUBLICATIONS 3,915 CITATIONS

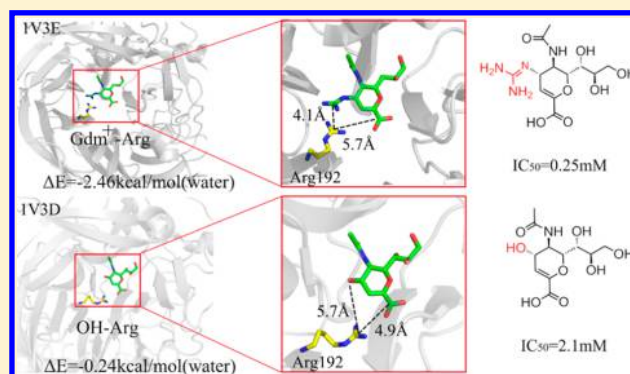
SEE PROFILE

Like-Charge Guanidinium Pairing between Ligand and Receptor: An Unusual Interaction for Drug Discovery and Design?

Yang Yang,[†] Zhijian Xu,^{*,†,§} Zhengyan Zhang,^{†,||} Zhuo Yang,[†] Yingtao Liu,[†] Jinan Wang,[†] Tingting Cai,[†] Shujin Li,^{||} Kaixian Chen,[†] Jiye Shi,^{*,‡} and Weiliang Zhu^{*,†}[†]CAS Key Laboratory of Receptor Research, Drug Discovery and Design Center, Shanghai Institute of Materia Medica, Chinese Academy of Sciences, Shanghai 201203, China[‡]Informatics Department, UCB Pharma, 216 Bath Road, Slough SL1 4EN, United Kingdom[§]State Key Laboratory of Medicinal Chemical Biology, Nankai University, 94 Weijin Road, Nankai District, Tianjin 300071, China^{||}College of Chemistry, Chemical Engineering and Materials Science of Soochow University, Soochow University, Suzhou, Jiangsu 215123, China

S Supporting Information

ABSTRACT: A database survey in this study revealed for the first time that there are 227 counterintuitive like-charge guanidinium pairings (Gdm⁺–Arg pairings) between ligands and receptors in the Protein Data Bank, implying the potential guanidinium–arginine binding between guanidine-containing drugs and their target proteins. Furthermore, there are 145 guanidine-containing molecules in the DrugBank, showing the prevalence of guanidinium groups in drugs. It has also been reported that the introduction of a guanidinium group forming Gdm⁺–Arg pairing improved the potency of the drug by more than 8-fold in a typical case. On the basis of the survey, six ligand–protein complexes with typical Gdm⁺–Arg pairings were chosen for QM/MM calculations. The calculations at the B97-D/6-311++g(d,p) level revealed that the interaction could be as strong as –1.0 to –2.5 kcal/mol in DMSO and water, comparable to common intermolecular interactions. The calculations also unveiled that the Gdm⁺–Arg pairing interactions change from repulsive to attractive with the increase of dielectric constant, suggesting that the dielectric constant has a general stabilization effect on the Gdm⁺–Arg pairing. This study suggested that the like-charge guanidinium pairing interaction could be used not only for tuning the physical and chemical properties of drug leads but also for improving ligand binding affinity.



1. INTRODUCTION

Guanidine is a strong organic base under physiological conditions, whereas its conjugate acid, guanidinium cation (Gdm⁺), is rather weak with a pK_a value of 13.6.¹ Due to the special chemical and physical properties of the guanidinium group, compounds with a guanidinium moiety possess various activities, e.g., anticancer, antidiabetic, antithrombotic, chemotherapeutic, and anti-inflammatory activities, and they are also able to act within the central nervous system.^{2–4} For example, metformin is the most widely used antidiabetic that belongs to the biguanide class. Hydroxyguanidine is an antitumor drug.⁵ Some guanidine-based compounds are neuraminidase inhibitors, which exhibit antiviral efficacy in avian and pandemic influenza.^{6,7} Diketopiperazine derivatives containing the guanidine functional group were evaluated as selective tryptase inhibitors.⁸ Therefore, the guanidinium group has attracted a great deal of attention in the past several decades in the field of drug discovery and development.

The guanidinium group is indispensable for many drugs' therapeutic effect, e.g., antihyperglycemic and antimalarial effect

of biguanides. If there are arginine residues in the binding site, the possible positive-positive charge interaction of Gdm⁺–Arg between the guanidine-containing drug and target might be thought to be repulsive due to the like-charge interaction, leading to decrease of bioactivity.

It was found that two positively charged guanidinium groups in protein are possibly attractive to each other within a short distance.^{9–13} Monte Carlo simulations revealed a counterintuitive attraction of the like-charge guanidinium–guanidinium (Gdm⁺–Gdm⁺) ion pairings with interaction (C···C) distance less than 5.0 Å.¹⁰ The attraction may come from induced solvent effects, which could overcome the electrostatic repulsions in the gas phase.¹⁰ *Ab initio* molecular dynamics simulations attributed the attraction primarily to the amphiphilic behavior of the guanidinium cation and van der Waals interactions between the cations.¹⁴ A control simulation

Received: April 30, 2015

Revised: August 18, 2015

Published: August 19, 2015

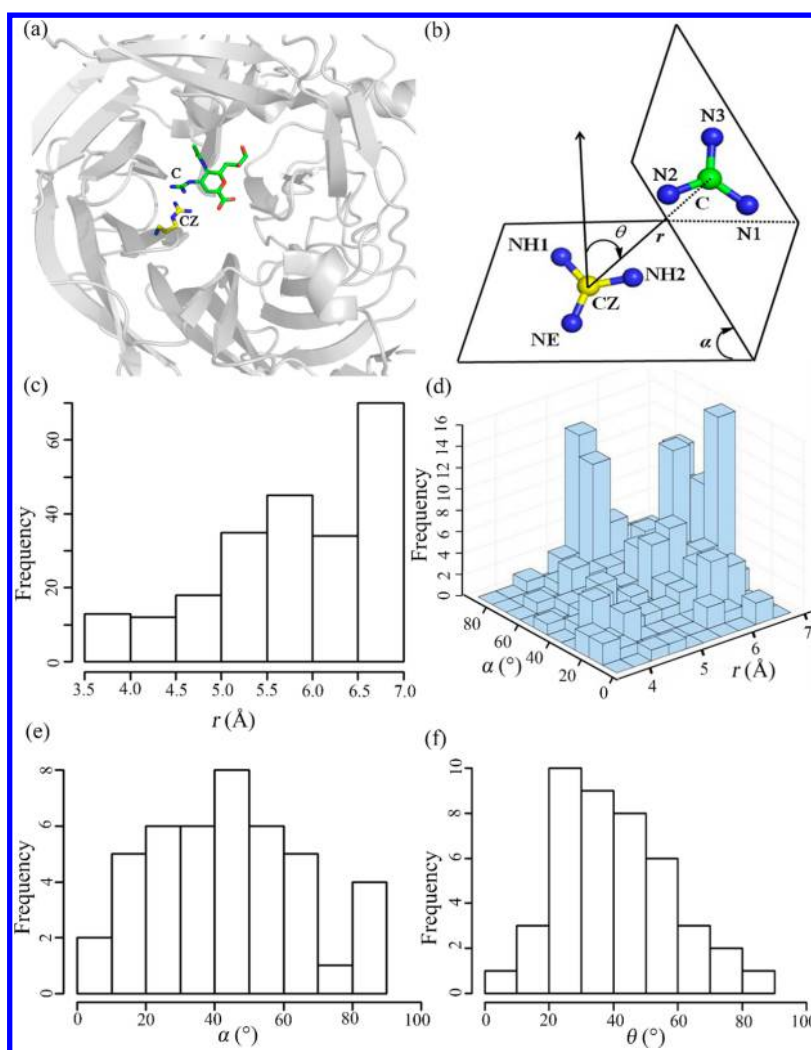


Figure 1. Gdm⁺–Arg interactions in the PDB. (a) A selected example of Gdm⁺–Arg pairing. Zanamivir (4-GU-DANA) and Arg192 form a stable pair with a C...CZ distance of 4.28 Å in hPIV-3neuraminidase (PDB code: 1V3E). (b) Geometric parameters of the Gdm⁺–Arg interaction. The definition for C...CZ distance r , interplanar angle α , and angular displacement θ . (c) r distribution for 227 pairs of Gdm⁺–Arg interactions with $r < 7$ Å. (d) r and α distribution for 227 pairs of Gdm⁺–Arg interactions with $r < 7$ Å. Frequency distributions of 43 Gdm⁺–Arg pairings with $r < 5$ Å for α (e), and θ (f).

on two like-charge ammonium cations did not show such counterintuitive attraction, which provided strong evidence for the specificity of the like-charge Gdm⁺–Gdm⁺ pairing.¹⁴ The *ab initio* molecular orbital calculations by polarizable continuum model (PCM) demonstrated that the guanidinium pairs were stably formed at staggered, eclipsed, and perpendicular conformations in aqueous solution whereas they were repulsive in the gas phase. It was proposed that van der Waals interactions contribute little to the guanidinium pairing attraction whereas the stabilization effect by the solvent water contributes a lot to the attraction.¹¹ Similar to its behavior in water, Gdm⁺–Gdm⁺ was found to be stable through stacking interaction in guanidinium chloride solutions using the combination of neutron diffraction data and molecular dynamics simulations. It was found that the guanidinium ions exhibit a strong tendency to self-associate with chloride counterions around them.¹⁵

Analogous to the case of the guanidinium cation presented above, pairings of guanidinium moieties of short arginine-rich peptides were found to be stably formed with the help of explicit molecular dynamics simulations and PCM *ab initio*

calculations. The cavitation (solvent exclusion) energy and dispersion interactions between guanidinium moieties account for the attraction based on the *ab initio* energy decomposition.¹⁶ In addition, structural database surveys also revealed the existence of the like-charge guanidinium pairings. For example, in the year 1993, 41 arginine-arginine pairs with CZ...CZ distances (r) less than 5 Å were discovered in the Protein Data Bank (PDB), with most of them residing in the vicinity of protein surfaces.¹⁷ In 1997, by analyzing 1680 nonredundant representative PDB structures, it was found that stacked conformation of guanidinium pairing is preferred when $3 \text{ Å} \leq r < 4 \text{ Å}$, whereas the T-shaped conformation is preferred when $4 \text{ Å} \leq r < 5 \text{ Å}$.¹⁸ In 2008, in a PDB data set of 266 protein dimers, 22% of arginines form guanidinium pairings, among which 77% of the pairings are located on protein interface, implying that guanidinium pairing might serve as a driving force in protein–protein interaction.¹³ In 2009, with the help of the program Atlas of Protein Side-Chain Interactions,¹⁹ six distinct structural motifs of guanidinium pairing in the PDB were detected, mostly in stacking-like arrangements.¹² In 2011, a PDB survey revealed that the stacking of guanidinium groups in Arg–Arg

Table 1. Six Selected Ligand–Receptor Complexes with Gdm⁺–Arg Pairing from PDB and the Comparisons between the X-ray Structures and the Optimized Ones

proteins	PDB ID	ligand		C...CZ (Å)	α (deg)	θ (deg)	RMSD (Å)
HIV-1 protease	1K2C	0Q4	X-ray	3.70	12.8	35.4	0.87
			optimized	3.69	19.2	20.7	
TiaS	3AU7	AG2	X-ray	3.77	27.3	22.3	1.29
			optimized	3.41	16.6	22.1	
HIV-1 protease	2AVQ	2NC	X-ray	3.92	42.9	41.7	0.96
			optimized	3.79	15.9	35.1	
RNase A	1RBW	GAI	X-ray	4.51	22.1	15.0	0.99
			optimized	3.92	32.5	14.9	
HIV-1 protease	2AVM	2NC	X-ray	4.75	82.8	60.6	1.04
			optimized	4.53	27.1	46.7	
HN glycoprotein	1V3E	ZMR	X-ray	4.05	22.8	16.0	0.89
			optimized	3.98	25.4	14.2	

dipeptides is completely due to structured protein constrains whereas the stacking of guanidinium groups in Arg–X–Arg tripeptides is not.¹⁶ A systematic PDB survey manifested that arginine–arginine pairing (Arg–Arg) resided in about one-third of the protein structures.²⁰ In 2012, a survey of over 70 thousand PDB structures showed that Arg–Arg is commonly found in protein–protein oligomerization.²¹ Furthermore, a Cambridge structural database (CSD) survey also revealed the existence of the guanidinium pairing.¹⁸

Nevertheless, all the results shown above are about the interactions of the Gdm⁺–Gdm⁺ pairing merely in small molecules or proteins. Recently, the pairing between dissolved guanidinium and arginine side chains was observed by a combination of capillary electrophoresis experiments and MD simulations.²² Given the above contexts, we naturally asked whether a like-charge guanidinium pairing could be formed between a ligand and a receptor. To explore this problem, we employed a combined PDB survey and hybrid ONIOM (our own *n*-layered integrated molecular orbital and molecular mechanics, QM/MM)^{23–25} study. In a special case of Gdm⁺–Arg interaction, where 2,3-dehydro-2-deoxy-*n*-acetyl neuraminic acid (DANA) was changed to 4-GU-DANA (zanamivir) by introducing a guanidinium moiety into DANA, activity against the neuraminidase of human parainfluenza virus type 3 (hPIV-3) was significantly improved by 8.4 fold.^{26–28} The X-ray structure suggested that the like-charge guanidinium pairing could be formed between the new ligand and its target protein. Thus, the introduction of the guanidinium group into a drug is beyond the traditional role of changing physicochemical properties, it could also be used to improve binding affinity. Therefore, this unusual like-charge guanidinium pairing between a ligand and a receptor could be utilized in drug discovery and design for improving both drugability and bioactivity of lead compounds.

2. MATERIALS AND METHODS

2.1. Database Survey. The PDB database (up to March 2015), containing 107 436 structures, was used to explore the Gdm⁺–Arg pairing between ligands and proteins. First, the ligand substructure query against the PDB database using smiles NC(N)=N yielded 881 pdb structure hits. Second, an OpenBabel script was used to determine the guanidinium group in ligand sdf file. If a carbon atom bonded to three nitrogen atoms with bond orders of two, one, and one, it might be a guanidinium group. Then, visual inspection was employed to identify the real guanidinium group. Finally, a PyMOL script

was utilized to determine the geometric parameters of the Gdm⁺–Arg pairing, i.e., distance *r*, interplanar angle α , and angular displacement θ (Figure 1b). On the basis of α , the guanidinium–guanidinium interactions were termed as parallel ($0^\circ \leq \alpha \leq 30^\circ$), oblique ($30^\circ < \alpha \leq 60^\circ$), and perpendicular ($60^\circ < \alpha \leq 90^\circ$). As for θ , the Gdm⁺–Arg interactions were termed as centered ($0^\circ \leq \theta \leq 30^\circ$), offset ($30^\circ < \theta \leq 60^\circ$), and edge ($60^\circ < \theta \leq 90^\circ$).¹³

2.2. ONIOM Hybrid Calculations. On the basis of the PDB survey, six X-ray structures with guanidinium pairing between ligand and receptor (PDB ID: 1K2C, 3AU7, 2AVQ, 2AVM, 1RBW, and 1V3E) were retrieved from the PDB database for QM/MM calculation (Table 1). For 1V3E, there were two identical chains; only one was retained. Meanwhile, water molecules close to the binding sites of the guanidine ligands and the arginine residues were preserved but other water and small molecules were removed. The H++ web server for estimating pK_a²⁹ was utilized to add hydrogen atoms and calculate the protonation states of the protein residues.

QM/MM is a powerful and efficient method for the geometry optimization of large biological systems. The advantage of the QM/MM method is that atoms in the important “active site” of large biologically relevant systems can be treated with the accurate QM method while the remaining region can be treated with an inexpensive MM method.³⁰ A two-layer ONIOM³¹ scheme was performed for the protein–ligand interactions in this study. The guanidine ligands or the truncated ones (polypeptide-type ligands) (Figure 2) and the corresponding arginine residues that interact with the ligands were included in the QM region where the density functional theory (DFT) augmented with empirically parametrized dispersion corrections (DFT-D³²) B97-D^{33–35}/6-311++G(d,p) was employed, and the remaining atoms were included in the MM layer. The AMBER parm96 force field³⁶ was used for the MM layer and the TIP3P model^{37,38} was applied for description of the water molecules surrounding the protein. The partial charges of the ligands were calculated with a restricted electrostatic-potential (RESP) fitting procedure, which produced the charge of AMBER force field,³⁹ whereas the parameters that were not found in AMBER force field were chosen from the generalized amber force field (GAFF) package.⁴⁰ Dangling bonds between the QM and MM regions were treated with hydrogen link atoms^{41–43} accordingly. The electrostatic interactions between the two layers were treated with electronic embedding at the QM level as opposed to mechanical embedding at the MM level.^{42,44}

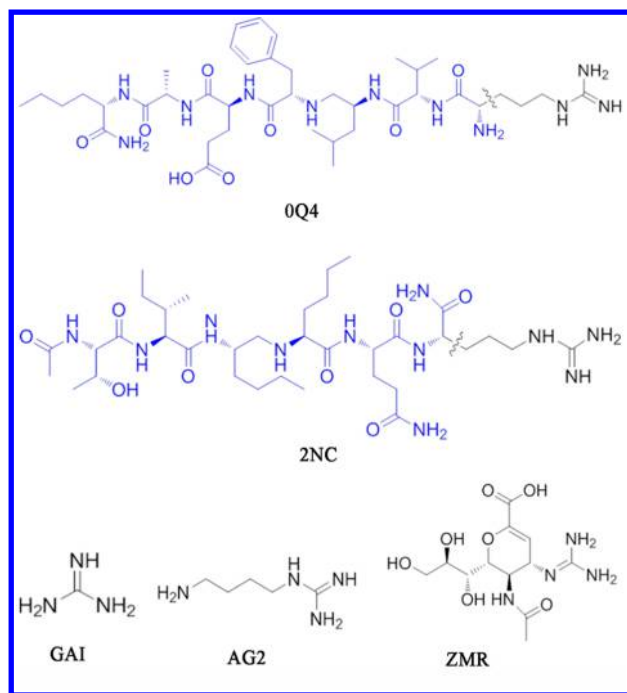


Figure 2. Chemical structures of the ligands in six model systems. The waved line is the site where the ligand was truncated for the calculations in this study. The guanidinium ligands or the truncated ones (when the ligand is polypeptide) and the corresponding side chains of arginine residues that interact with the ligands were included in the QM layer, and the rest was put in the MM layer.

To explore the solvation effect on the ligand binding sites, the QM layers of each of the six complexes were extracted for single-point energy calculations. Considering the anisotropic and inhomogeneous dielectric properties of proteins,^{45,46} single-point PCM solvation energy^{47,48} calculations were performed in chloroform ($\epsilon = 4.8$), acetone ($\epsilon = 20.5$), DMSO ($\epsilon = 46.8$), and water ($\epsilon = 78.4$) at the B97-D/6-311++G(d,p) and MP2/6-311++G(d,p) level. All these calculations were carried out with the *Gaussian 09* program package.⁴⁹

3. RESULTS AND DISCUSSION

3.1. Guanidine-Containing Drugs in DrugBank. There are 145 guanidine-containing compounds in the DrugBank⁵⁰ (Table S1 and Table S2, Supporting Information) as of April 2015. The molecular weights of the 145 drugs have been sorted into a histogram (Figure 3b), with the distribution of small molecule drugs and polypeptide drugs shown in green and blue, respectively. It can be seen that the maximum distributed range of the molecular weight is between 200 and 300, which falls into that of small molecule drugs. This may indicate that compounds with guanidine of large molecular weight except peptides are of poor ADME/T property. As the molecular weight rises, the amount of the polypeptide drugs increases quickly. The chemical structures of some well-known drugs with guanidiniums are also shown in Figure 3.

Zanamivir, a guanido-neuraminic acid, is an orally inhaled drug for the treatment and prophylaxis of human influenza virus infection.⁵¹ It is a neuraminidase inhibitor by mimicking sialic acid which is the natural substrate of the neuraminidase, leading to inactivation of virus in escaping its host cell and infecting others.⁵² Studies have shown that zanamivir has a good safety profile when initiated early.⁵³ There are many other drugs with guanidinium functional groups in the DrugBank. Metformin, the most widely prescribed antihyperglycemic drug, is a biguanide agent with a pK_a of 12.4 that helps control blood sugar levels in patients with non-insulin-dependent diabetes mellitus (NIDDM). Another well-known guanidine derivative is bethanidine, with a pK_a value of 10.6,⁵⁴ which functions as an effective antihypertensive agent.⁵⁵ Amiloride, a pyrazine-carbonyl-guanidine with a pK_a value of 8.7, is used as a potassium-sparing diuretic in the treatment of hypertension and edema. The guanidinium functional groups in these drugs are indispensable as they are essential for both bioactivity and the ADME/T properties of the drug molecules.

All the informations above imply a significant role of guanidinium groups in the drug market (Table S2, Supporting Information). In addition, guanidine exists as various substructures of natural products in biological systems. For example, it is present in arginine, guanine, and creatine. The special characteristics of basicity of the guanidine cation endow it various functions in biological systems. The guanidinium ion

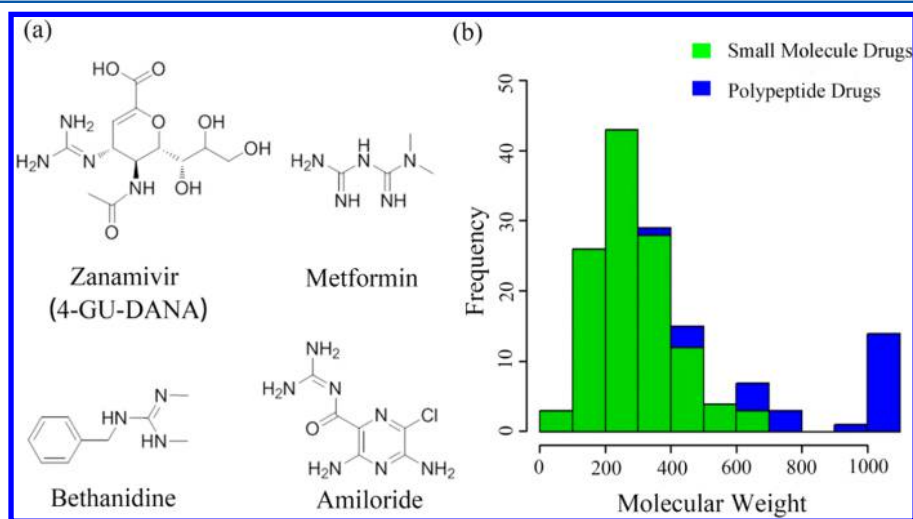


Figure 3. Guanidine-containing drugs in DrugBank. (a) Typical chemical structures of guanidine-containing drugs. (b) Molecular weight distributions of guanidine-containing drugs.

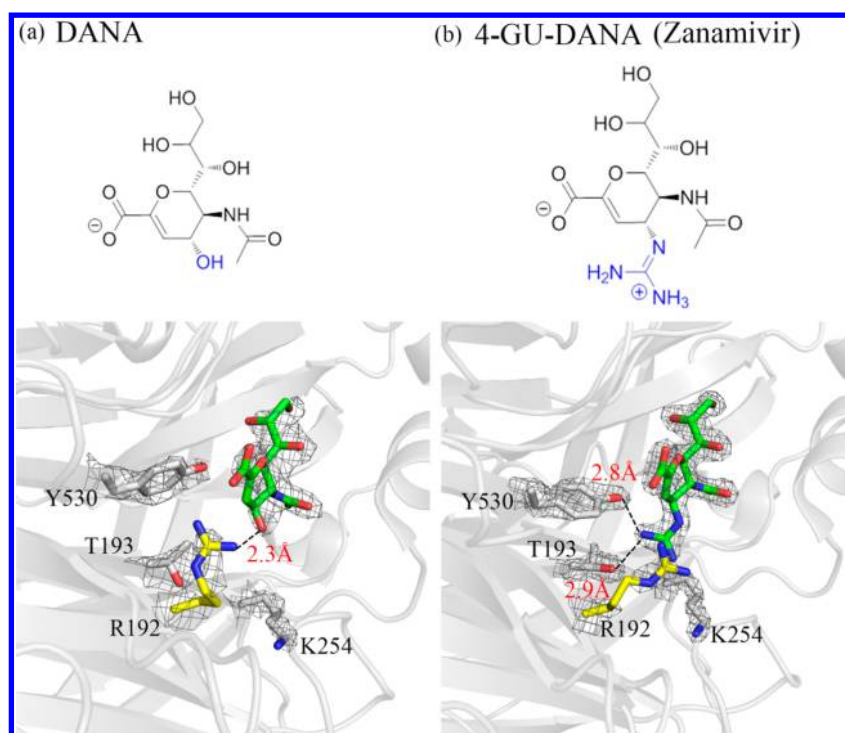


Figure 4. Chemical structures of two neuraminidase inhibitors without (a, PDB code 1V3D) or with guanidinium group (b, PDB code 1V3E) and their binding modes with hPIV3 neuraminidase. hPIV3 neuraminidase is shown in gray, residues within 5 Å of the 4-GU-DANA(Zanamivir) guanidinium group are shown in sticks, and the electron density maps are contoured at 1.0σ .

can associate with aromatic amino acid side chains of protein and form strong hydrogen bonds with water and polar side chains simultaneously, which is often used as an effective protein denaturant.¹⁵ In addition, guanidine derivatives have been found to be nontoxic and efficient disinfectants or additives, which are widely used in daily life.^{56,57} Polyguanidines are safe biocides with good effects and low toxicity, which can be rapidly attracted to bacterial surface, leading to irreversible loss and leakage of important components of a bacterial cell, consequently causing a great damage to the cytoplasmic membrane. Another major reason to include guanidinium into a drug might be its potential role in facilitating cellular uptake.⁵⁸ Therefore, the guanidine derivatives have great potential to be promising novel drugs.

3.2. Gdm⁺–Arg Pairing in PDB. Statistical analysis of the Gdm⁺–Arg pairings in the PDB may shed some light on the importance of such interaction in biological systems. After misordered guanidinium groups were removed, 718 ligands with guanidinium groups have been found in 661 PDB structures. There are 227 Gdm⁺–Arg pairings with C...CZ distances (r) less than 7 Å in PDB. Figures 1c and 1d show that there are two peaks for r , one near 5.75 Å with α between 70 and 90°, another peak near 6.8 Å with α between 40 and 70°, showing a bimodal distribution for r values. If the distance frequency distribution was normalized with $4\pi r^2$, a similar bimodal distribution was observed (Figure S1(a), Supporting Information). There are 43 Gdm⁺–Arg pairings showing an r value less than 5 Å, suggesting that at least 6.0% (43/718) guanidine ligands could form Gdm⁺–Arg pairings. Electron-density maps of these 43 Gdm⁺–Arg pairings have been examined, among which 24 maps (56%) are available and eight systems of 1K2C, 3AU7, 1V3E, 2IHV, 3CKZ, 3U4F, 1FOJ, and 4AM8 have clear maps of Gdm⁺–Arg pairings that are shown

in Figure S2 (Supporting Information). These results suggest that the Gdm⁺–Arg pairing should exist in biological systems.

Compared to the 4 Å peak of the Gdm⁺–Gdm⁺ pairings and the Arg–Arg pairings,^{15,20} the first peak of the Gdm⁺–Arg pairings is about 1 Å longer in distance, which is not unexpected, considering the much higher complexity of biomacromolecules. The relatively flat α distribution within 5 Å of r suggests that parallel Gdm⁺–Arg pairings may not be so dominant any more between ligands and proteins in ligand–receptor complexes (Figure 1e), which differs from the cases of the Gdm⁺–Gdm⁺ pairings¹⁴ and the Arg–Arg pairings.²⁰ Therefore, the surroundings around ligand binding sites may have a striking influence on the geometries of Gdm⁺–Arg pairings. The normalized α angle frequency distribution (frequency/ $\sin(\alpha)$) (Figure S1(b), Supporting Information) was similar to that without correction, with the peak shifted from 30° to 40°. The θ distribution with r less than 5 Å has a peak near 30°, which accords with the reported off-center Arg–Arg orientation.²⁰ There are 13 Gdm⁺–Arg pairings with $r < 4$ Å found in PDB, showing much stronger interactions between the guanidine-containing ligand and protein, which are mainly parallel and oblique conformations (Table S3, Supporting Information). The obvious variation in the configurations of the Gdm⁺–Arg pairings found in receptor–ligand complexes from the Arg–Arg pairings in proteins indicates that great complication should be considered in rational guanidine drug design.

Microenvironment around the Gdm⁺–Arg Pairing. Residues within 5 Å of the 43 Gdm⁺–Arg pairings with $r < 5$ Å have been examined in this study (Figure S3, Supporting Information). The results here are in agreement with the previous reports that indicated oxygen atoms of water play an important bridging role in stabilizing like-charge ion pairing¹⁷ and that anionic Asp and Glu, and aromatic Tyr, Phe, and Trp

as well as Leu, Lys, and Met tend to occur within 10 Å of Arg–Arg pairings.¹³ We found that water is of the highest occurrence, accounting for more than 32% of all the surrounding residues. In addition, about 27% of the residues are Asp, showing a rather high frequency, which indicates the Gdm⁺–Arg pairing could form salt bridges with such anionic residue. It is clear that the like-charge Gdm⁺–Arg pairing tends to occur in a relatively polar environment (Figure S3), which is in accordance with our previous findings.²⁰

Protonation State of Gdm⁺–Arg Pairing. pK_a values of the Gdm⁺–Arg pairings of the 43 PDB structures with *r* < 5 Å are predicted by the PROPKA program.^{59–62} The pK_a values of all of the arginine residues are higher than 9.00 (Table S4, Supporting Information), suggesting that they are protonated in the protein environment. With regard to the ligand, the lowest pK_a value of the guanidinium group is 9.96 (PDB code: 3NYG), which implies a protonated state. Therefore, all of the Gdm⁺–Arg pairings in the 43 structures should be like-charged.

3.3. Gdm⁺–Arg Pairing To Enhance Drug's Efficacy.

The virus hPIV-3 is a leading cause for lower respiratory tract infections in children, with no approved drug available to date.⁶³ The hPIV-3 neuraminidase is a promising target with its essential role in the virus' life cycle. DANA was found to inhibit hPIV-3 neuraminidase with IC₅₀ value of 2.1 mM. When the hydroxyl group on the C-4 carbon was substituted with a guanidinium group, it became 4-GU-DANA (Zanamivir), an approved drug for the treatment of infections caused by influenza A and influenza B. Impressively, the IC₅₀ of zanamivir against hPIV-3 neuraminidase was 0.25 mM, 8 times more active than that of DANA (IC₅₀ = 2.1 mM).²⁷ The cocrystal structures of DANA/zanamivir and hPIV-3 neuraminidase were carefully inspected.²⁸ Figure 4 shows that the enhanced efficiency of zanamivir introduced by the guanidinium group should be attributed to two factors. First, the guanidinium group of R192 flipped toward the C-4 guanidinium group to form a typical and stable Gdm⁺–Arg pairing in the zanamivir/neuraminidase complex (PDB code: 1V3E) with C···CZ distances of 4.05 Å in chain A and 4.28 Å in chain B, respectively. Second, Y530 and T193 also flipped toward the C-4 guanidinium group to form hydrogen bonds, compared to the structure of DANA/neuraminidase complex (PDB code: 1V3D). When the guanidinium group of the ligand is substituted by an amino group, it becomes 4-AM-DANA (4-amino-Neu5Ac2en), which is the least effective inhibitor among the three (IC₅₀ is 3.2–8.0 mM).²⁷ The binding energies between the NH₄⁺ of 4-AM-DANA and Arg192 of hPIV-3 neuraminidase were calculated to be +0.31 kcal/mol in DMSO and −0.24 kcal/mol in water, respectively (Table 2). On the contrary, the energies between the Gdm⁺ of 4-GU-DANA (Zanamivir) and Arg192 are −1.96 kcal/mol in DMSO and −2.46 kcal/mol in water, respectively, showing that guanidinium is different from the ammonium ion in nature, which reveals the important role of the Gdm⁺–Arg pairing in drug-target binding affinity.

3.4. Structures of the Optimized Gdm⁺–Arg Pairings.

The optimized QM layer for six typical systems at the level of ONIOM (B97-D/6-311++G(d,p):AMBER)²⁰ and the corresponding X-ray structures are given in Figure 5. Data of the optimized geometries and RESP charges for the ligand and Amber charges for the protein are also provided in the Supporting Information. The root-mean-square derivation (RMSD) values of the optimized QM layer structures relative to their X-ray structures are determined to be 0.9–1.3 Å, which

Table 2. Binding Energies (kcal/mol) of Gdm⁺–Arg Pairing and NH₄⁺–Arg Pairing (4-AM-DANA), Calculated by B97-D/6-311++G(d,p) in a Vacuum ($\epsilon = 1.0$) and a Series of Solvents (Chloroform, $\epsilon = 4.8$; Acetone, $\epsilon = 20.5$; DMSO, $\epsilon = 46.8$; Water, $\epsilon = 78.4$)

system	vacuum (BSSE ^a)	chloroform	acetone	DMSO	water
1K2C	58.36 (0.58)	11.60	0.91	−0.99	−1.59
3AU7	60.57 (1.17)	11.95	1.45	−0.38	−0.96
2AVQ	56.29 (0.72)	10.17	0.05	−1.70	−2.25
1RBW	56.79 (0.49)	10.14	0.17	−1.54	−2.08
2AVM	52.97 (0.45)	9.92	0.31	−1.36	−1.89
1V3E	51.80 (0.70)	9.56	−0.20	−1.92	−2.46
4-AM-DANA	52.94(0.44)	11.79	2.03	0.31	−0.24

^aBSSE stands for the basis set superposition errors.

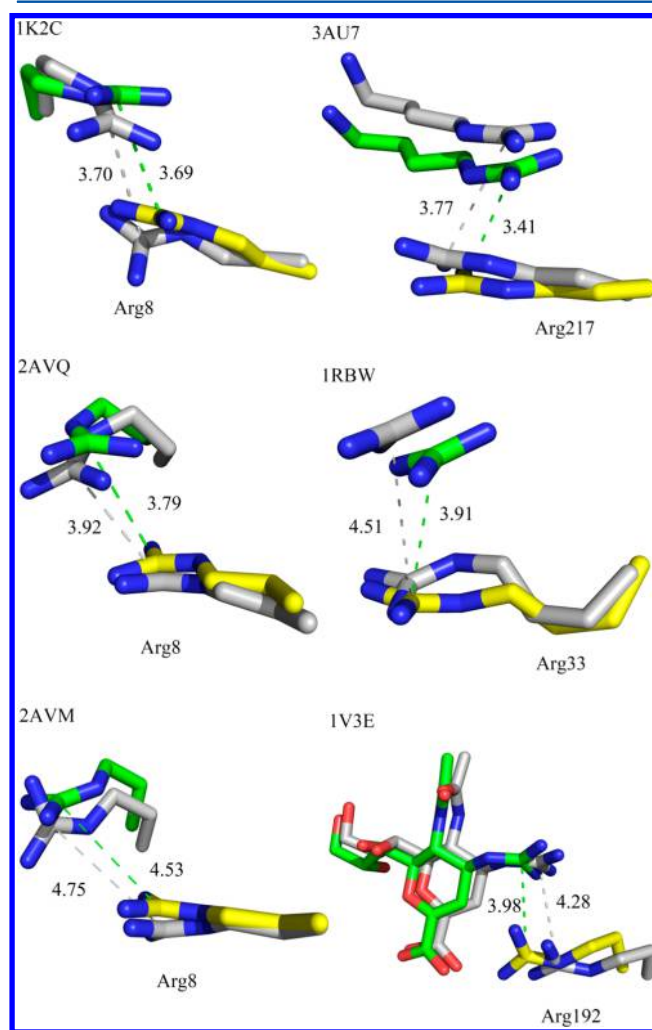


Figure 5. Gdm⁺–Arg pairings of the QM layer of the six model systems. Superimposition of X-ray structures (gray) and ONIOM (B97-D: AMBER) optimized structures (green, ligand part; yellow, arginine side chains of the protein). Distances between the central carbon atoms of the ligand and arginine are shown in angstroms.

quantify a small deviation of the optimized structures from their X-ray structures, indicating that the optimized models should be reliable (Table 1). It can be seen that the C···CZ distances of the Gdm⁺–Arg pairings in the optimized structures fall within a range of 3.57–4.54 Å, which is in agreement with the

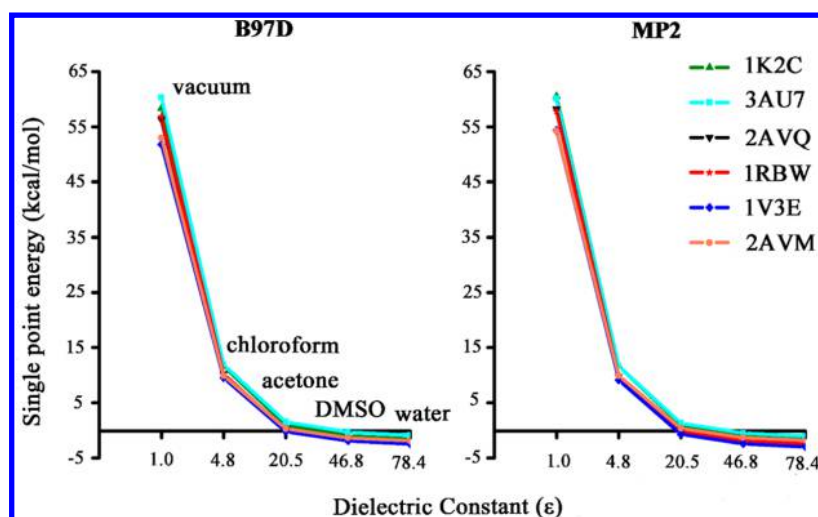


Figure 6. Binding energies calculated by B97-D/6-311++G(d,p) and MP2/6-311++G(d,p) methods of Gdm⁺–Arg pairings in a vacuum ($\epsilon = 1.0$) and a series of solvents (chloroform, $\epsilon = 4.8$; acetone, $\epsilon = 20.5$; DMSO, $\epsilon = 46.8$; water, $\epsilon = 78.4$).

experimentally determined values in crystal structures (3.70–4.75 Å). These separations, which are smaller than the sums of van der Waals radii of the atoms, show a possible component of van der Waals interaction in the pairings.¹³ In addition, to explore whether the initial ONIOM model is stable in the explicit water model, a 5 ns MD simulation was performed (detail simulation protocols were shown in [Supporting Information](#)). A hierarchical clustering analysis was performed on snapshots extracted from the equilibrium trajectory (1–5 ns) to obtain the representative structure using the kclust algorithm available in the MMTSB Tool set.⁶⁴ The results (Figure S4, [Supporting Information](#)) revealed that the representative structure of the equilibrium conformation was very similar to the parallel conformation used in the initial ONIOM calculation, especially for the high layer atoms (RMSD = 1.4 Å). Meanwhile, the C...CZ distance was kept at 4.00 Å in the representative structure, which is very near the distance of the initial ONIOM calculation (4.28 Å).

The Gdm⁺–Arg pairings in the structures of 1K2C, 2AVQ, 2AVM, and 1RBW are all located on the protein surfaces, which are surrounded by carboxyl groups and water molecules. Statistics show that positively charged arginine residues often reside on the protein surface where the dielectric constant is almost approaching that of the solvent.⁶⁵ As shown in [Table 1](#), the conformations of the above four Gdm⁺–Arg pairings are roughly parallel in the X-ray structures, and they are also parallel in the optimized structures ($\alpha < 30^\circ$), which can be mainly attributed to the polar environment with high dielectric constant.¹⁷ In a special case where two alternative ligand conformations are in the crystal structure of 2AVM (Figure S5, [Supporting Information](#)), one of the Gdm⁺–Arg conformations is parallel ($\alpha = 11.6^\circ$), whereas the other is perpendicular ($\alpha = 82.8^\circ$). The perpendicular one was selected as the initial structure for geometry optimization. It turned out that the perpendicular pairing was optimized to be parallel ($\alpha = 27.0^\circ$) at the ONIOM (B97-D/6-311++G(d,p): AMBER) level of theory. We checked the pdb structure again and found that the parallel conformation of the guanidinium group in the crystal structure of 2AVM has a bigger occupancy value (0.52, which refers to the relative frequency of occurrence for the certain conformer in the crystal) and a smaller *b* factor value (average value 19.4) than the perpendicular one (occupancy 0.48 and

the average *b* factor value 27.2), which suggests that the parallel configuration may occur more frequently in the biological systems, in accordance with the QM/MM optimization result. As the guanidinium group resides on the surface of the protein in 2AVM, it is not surprising to find that the parallel conformation is preferred in this case, which is consistent with our previous study for Arg–Arg pairings.²⁰

The Gdm⁺–Arg pairings of 3AU7 and 1V3E are partially buried in the proteins. However, due to the water molecules and polar groups such as hydroxyl and carboxylate groups around the pairings, the dielectric constant of the micro-environment of the Gdm⁺–Arg pairings is relatively higher than that of the interior protein, providing a polar environment for the interaction between guanidinium group and arginine residue. This may explain why they also occur as parallel pairings. The QM/MM optimization results show that parallel conformations of the Gdm⁺–Arg pairings are favorable in all of the six model systems with α values less than 30° , owing to the polar microenvironment around the pairings.

It should be pointed out that the six examples here do not represent all the situations in biological systems. Nevertheless, the study here takes a deeper look into the special like-charge Gdm⁺–Arg pairing and may give some information on this kind of interaction in rational drug design.

3.5. Energies of the Optimized Gdm⁺–Arg Pairings. In this paper, we focus on the interaction energy between the ligand-containing guanidinium group and the arginine in the receptor protein to describe the ligand binding affinity. In general, the more negative the interaction energy, the stronger the binding affinity. Single-point PCM solvation energy calculations were performed using the B97-D/6-311++G(d,p) method in chloroform, acetone, DMSO, and water, respectively ([Table 2](#)). The MP2/6-311++G(d,p) method was also applied in these systems for further validation, which yielded similar binding energies ([Figure 6](#) and [Table S5](#), [Supporting Information](#)), indicating that the results from the B97-D/6-311++G(d,p) method are reliable. If the BSSE (basis set superposition errors) is considered, the result is consistent with the current conclusion ([Figure S6](#), [Table S6](#), [Supporting Information](#)). Therefore, the result from B97-D/6-311++G(d,p) calculations ([Table 2](#)) was utilized in the following discussions. The interaction energies between the guanidinium

group of the ligand and arginine are positive in a vacuum and can be as large as 50–60 kcal/mol, indicating that the pairings are not stable in a vacuum ($\epsilon = 1$) because strong electrostatic repulsion exists between the like-charge ion pairs.¹⁷ However, with the increase of the dielectric constant, the repulsive strengths of the interaction between the Gdm⁺–Arg pairings become weaker. For instance, in 1K2C, the binding energy is 58.36 kcal/mol in a vacuum ($\epsilon = 1$), but it declines to 11.60 kcal/mol in chloroform ($\epsilon = 4.8$). Moreover, the energy falls to 0.91 kcal/mol in acetone ($\epsilon = 20.5$). Impressively, the interaction energies of all the Gdm⁺–Arg pairings become negative in DMSO ($\epsilon = 46.8$), showing attractive interactions. The calculated binding energies for the six systems range from –1.0 to –2.5 kcal/mol in highly polar environments like DMSO and water, which are comparable to energies of other intermolecular interactions, e.g., hydrogen bond, cation– π interaction, and halogen bonding.^{66,67} In summary, a high dielectric constant may have an essential stabilization effect on the like-charge Gdm⁺–Arg pairings. To further explore the binding characteristic, a decomposition analysis on binding energy was performed with ADF2013, the result suggested that solvation effect might play key role in the like-charge Gdm⁺–Arg pairing (Figure S7 and Table S7, Supporting Information).

4. CONCLUSIONS

Despite the limited extent of this study on like-charge guanidinium pairing, it could be concluded that the interaction of Gdm⁺–Arg pairing can be formed between ligand and receptor. A DrugBank survey showed the prevalence of the guanidinium group in the drugs, which led us to explore the potential role of guanidinium pairing in the biology world. For the first time, a systematic PDB survey exposed the existence of the like-charge guanidinium pairing interactions between the guanidine ligand and protein arginine residue, indicating its important role in ligand recognition and binding. Specifically, it has also been reported that the introduction of the guanidinium group improved zanamivir's potency 8.4 times against hPIV-3 neuraminidase, and the binding energies between Gdm⁺–Arg pairing in this paper were also calculated to be –1.92 kcal/mol in DMSO and –2.46 kcal/mol in water, showing strong attraction under such conditions. ONIOM-based QM/MM calculations on six typical systems confirmed the stabilization of these nonbonding like-charge guanidinium pairings. Furthermore, these pairings were found to be attractive in high dielectric constant solvents ($\epsilon > 46.8$) by single-point energy computations on the six model systems. We found that with the increase of the dielectric constant, a decreasing trend for the binding energy of the Gdm⁺–Arg pairings was observed, showing attractive interactions in DMSO ($\epsilon = 46.8$) in all systems. The calculated binding energy might be as strong as –1.0 to –2.5 kcal/mol in high dielectric constant solvents, which is comparable to that of other intermolecular interactions. The results in this work would help establish the concept of the like-charge guanidinium pairings as potential and effective nonbonding interactions for improving bioactivity and druggability of lead compounds in the field of drug discovery and design.

■ ASSOCIATED CONTENT

Supporting Information

The Supporting Information is available free of charge on the ACS Publications website at DOI: 10.1021/acs.jpcb.5b04130.

MD simulation protocols, solvation energies, and energy decomposition analysis (EDA) for Gdm⁺–Arg pairings, Tables S1–S7 containing molecular weights of guanidine-containing drugs, a list of guanidine-containing drugs, geometrical information for pairs of Gdm⁺–Arg interactions, pK_a values, binding energies, and energy components, and Figures S1–S7 illustrating pairing frequency vs distance, electron-density maps, residues occurring within a 5 Å cutoff of Gdm⁺–Arg pairings, Gdm⁺–Arg pairings, alternative ligand conformations, binding energies of Gdm⁺–Arg pairings, and energy components (PDF)

Optimized geometries and RESP charges for the ligand and Amber charges for the proteins (PDF)

■ AUTHOR INFORMATION

Corresponding Authors

*Z. Xu. Phone: +86-21-50806600-1201. E-mail: zjxu@sim.ac.cn.

*J. Shi. Phone: +32-2-3862861. E-mail: Jiye.Shi@ucb.com.

*W. Zhu. Phone: +86-21-50805020. E-mail: wlzhu@mail.shcnc.ac.cn.

Notes

The authors declare no competing financial interest.

■ ACKNOWLEDGMENTS

This work was supported by National Natural Science Foundation of China (81273435 and 81302699), National High Technology Research and Development Program of China (2012AA01A305), National Science & Technology Major Project (2013ZX09103001-001 and 2012ZX09301001-004), China Postdoctoral Science Foundation (2014T70444), and the State Key Laboratory of Medicinal Chemical Biology, Nankai University (20130265).

■ REFERENCES

- (1) Kovacevic, B.; Maksic, Z. B. Basicity of Some Organic Superbases in Acetonitrile. *Org. Lett.* **2001**, 3 (10), 1523–1526.
- (2) Saczewski, F.; Balewski, L. Biological Activities of Guanidine Compounds. *Expert Opin. Ther. Pat.* **2009**, 19 (10), 1417–1448.
- (3) Saczewski, F.; Balewski, L. Biological Activities of Guanidine Compounds, 2008 - 2012 update. *Expert Opin. Ther. Pat.* **2013**, 23 (8), 965–995.
- (4) Orner, B.; Hamilton, A. The Guanidinium Group in Molecular Recognition: Design and Synthetic Approaches. *J. Inclusion Phenom. Mol. Recognit. Chem.* **2001**, 41 (1–4), 141–147.
- (5) Adamson, R. H. Biological Sciences: Hydroxyguanidine-a New Antitumour Drug. *Nature* **1972**, 236 (5347), 400–401.
- (6) Mishin, V. P.; Hayden, F. G.; Gubareva, L. V. Susceptibilities of Antiviral-Resistant Influenza Viruses to Novel Neuraminidase Inhibitors. *Antimicrob. Agents Chemother.* **2005**, 49 (11), 4515–4520.
- (7) Crusat, M.; de Jong, M. D. Neuraminidase Inhibitors and Their Role in Avian and Pandemic Influenza. *Antivir. Ther.* **2007**, 12 (4 Pt B), 593–602.
- (8) Fresno, M. d.; Fernández-Fórner, D.; Miralpeix, M.; Segarra, V.; Ryder, H.; Royo, M.; Albericio, F. Combinatorial Approaches towards the Discovery of New Trypsin inhibitors. *Bioorg. Med. Chem. Lett.* **2005**, 15 (6), 1659–1664.
- (9) Sheriff, S.; Silverton, E. W.; Padlan, E. A.; Cohen, G. H.; Smith-Gill, S. J.; Finzel, B. C.; Davies, D. R. Three-Dimensional Structure of an Antibody-Antigen Complex. *Proc. Natl. Acad. Sci. U. S. A.* **1987**, 84 (22), 8075–8079.
- (10) Boudon, S.; Wipff, G.; Maigret, B. Monte Carlo Simulations on the Like-charged Guanidinium-guanidinium Ion Pair in Water. *J. Phys. Chem.* **1990**, 94 (15), 6056–6061.

- (11) No, K. T.; Nam, K.-Y.; Scheraga, H. A. Stability of Like and Oppositely Charged Organic Ion Pairs in Aqueous Solution. *J. Am. Chem. Soc.* **1997**, *119* (S2), 12917–12922.
- (12) Vondrasek, J.; Mason, P. E.; Heyda, J.; Collins, K. D.; Jungwirth, P. The Molecular Origin of Like-Charge Arginine–Arginine Pairing in Water. *J. Phys. Chem. B* **2009**, *113* (27), 9041–9045.
- (13) Pednekar, D.; Tendulkar, A.; Durani, S. Electrostatics-defying Interaction between Arginine Termini as a Thermodynamic Driving Force in Protein–Protein Interaction. *Proteins: Struct., Funct., Genet.* **2009**, *74* (1), 155–163.
- (14) Vazdar, M.; Uhlig, F.; Jungwirth, P. Like-Charge Ion Pairing in Water: An Ab Initio Molecular Dynamics Study of Aqueous Guanidinium Cations. *J. Phys. Chem. Lett.* **2012**, *3* (15), 2021–2024.
- (15) Mason, P. E.; Neilson, G. W.; Enderby, J. E.; Saboungi, M.-L.; Dempsey, C. E.; MacKerell, A. D.; Brady, J. W. The Structure of Aqueous Guanidinium Chloride Solutions. *J. Am. Chem. Soc.* **2004**, *126* (37), 11462–11470.
- (16) Vazdar, M.; Vymetal, J.; Heyda, J.; Vondrasek, J.; Jungwirth, P. Like-Charge Guanidinium pairing from Molecular Dynamics and Ab Initio Calculations. *J. Phys. Chem. A* **2011**, *115* (41), 11193–11201.
- (17) Magalhaes, A.; Maigret, B.; Hoflack, J.; Gomes, J. N.; Scheraga, H. A. Contribution of Unusual Arginine–Arginine Short-Range Interactions to Stabilization and Recognition in Proteins. *J. Protein Chem.* **1994**, *13* (2), 195–215.
- (18) Soetens, J. C.; Millot, C.; Chipot, C.; Jansen, G.; Angyan, J. G.; Maigret, B. Effect of Polarizability on the Potential of Mean Force of Two Cations. The Guanidinium–Guanidinium Ion Pair in Water. *J. Phys. Chem. B* **1997**, *101* (50), 10910–10917.
- (19) Van Geerestein, V. J.; Ottenheijm, H. C. J. Atlas of Protein Side-Chain Interactions, Volumes I and II. *Trends Pharmacol. Sci.* **1992**, *14* (4), 133–134.
- (20) Zhang, Z.; Xu, Z.; Yang, Z.; Liu, Y.; Wang, J. a.; Shao, Q.; Li, S.; Lu, Y.; Zhu, W. The Stabilization Effect of Dielectric Constant and Acidic Amino Acids on Arginine–Arginine (Arg–Arg) Pairings: Database Survey and Computational Studies. *J. Phys. Chem. B* **2013**, *117* (17), 4827–4835.
- (21) Neves, M. A.; Yeager, M.; Abagyan, R. Unusual Arginine Formations in Protein Function and Assembly: Rings, Strings, and Stacks. *J. Phys. Chem. B* **2012**, *116* (23), 7006–7013.
- (22) Kubickova, A.; Krizek, T.; Coufal, P.; Wernersson, E.; Heyda, J.; Jungwirth, P. Guanidinium Cations Pair with Positively Charged Arginine Side Chains in Water. *J. Phys. Chem. Lett.* **2011**, *2* (12), 1387–1389.
- (23) Maseras, F. Hybrid Quantum Mechanics/Molecular Mechanics Methods in Transition Metal Chemistry. In *Organometallic Bonding and Reactivity*; Brown, J., Hofmann, P., Eds.; Springer: Berlin Heidelberg, 1999; Vol. 4, pp 165–191.
- (24) Gogonea, V. The QM/MM Method. An Overview. *Internet Electron. J. Mol. Des.* **2002**, *1* (4), 173–184.
- (25) Vreven, T.; Morokuma, K.; Farkas, O.; Schlegel, H. B.; Frisch, M. J. Geometry Optimization with QM/MM, ONIOM, and Other Combined Methods. I. Microiterations and constraints. *J. Comput. Chem.* **2003**, *24* (6), 760–769.
- (26) Levin Perlman, S.; Jordan, M.; Brossmer, R.; Greengard, O.; Moscona, A. The Use of a Quantitative Fusion Assay to Evaluate HN–Receptor Interaction for Human Parainfluenza Virus Type 3. *Virology* **1999**, *265* (1), 57–65.
- (27) Greengard, O.; Poltoratskaia, N.; Leikina, E.; Zimmerberg, J.; Moscona, A. The Anti-Influenza Virus Agent 4-GU-DANA (Zanamivir) Inhibits Cell Fusion Mediated by Human Parainfluenza Virus and Influenza Virus HA. *J. Virol.* **2000**, *74* (23), 11108–11114.
- (28) Lawrence, M. C.; Borg, N. A.; Streltsov, V. A.; Pilling, P. A.; Epa, V. C.; Varghese, J. N.; McKimm-Breschkin, J. L.; Colman, P. M. Structure of the Haemagglutinin-neuraminidase from Human Parainfluenza Virus Type III. *J. Mol. Biol.* **2004**, *335* (5), 1343–1357.
- (29) Gordon, J. C.; Myers, J. B.; Folta, T.; Shoja, V.; Heath, L. S.; Onufriev, A. H++: A Server for Estimating pKas and Adding Missing Hydrogens to Macromolecules. *Nucleic Acids Res.* **2005**, *33*, 368–371.
- (30) Suresh, C. H.; Vargheese, A. M.; Vijayalakshmi, K. P.; Mohan, N.; Koga, N. Role of Structural WaterMmolecule in HIV Protease-Inhibitor-Complexes: A QM/MM Study. *J. Comput. Chem.* **2008**, *29* (11), 1840–1849.
- (31) Dapprich, S.; Komáromi, I.; Byun, K. S.; Morokuma, K.; Frisch, M. J. A New ONIOM Implementation in Gaussian98. Part I. The Calculation of Energies, Gradients, Vibrational Frequencies and Electric Field Derivatives. *J. Mol. Struct.: THEOCHEM* **1999**, *461*–462 (0), 1–21.
- (32) Peverati, R.; Baldrige, K. K. Implementation and Performance of DFT-D with Respect to Basis Set and Functional for Study of Dispersion Interactions in Nanoscale Aromatic Hydrocarbons. *J. Chem. Theory Comput.* **2008**, *4* (12), 2030–2048.
- (33) Vazquez, M. A.; Sherrill, C. D.; Apra, E.; Sumpter, B. G. An Assessment of Density Functional Methods for Potential Energy Curves of Nonbonded Interactions: The XYG3 and B97-D Approximations. *J. Chem. Theory Comput.* **2010**, *6* (3), 727–734.
- (34) Yamashita, H.; Yumura, T. The Role of Weak Bonding in Determining the Structure of Thiophene Oligomers inside Carbon Nanotubes. *J. Phys. Chem. C* **2012**, *116* (17), 9681–9690.
- (35) Wu, J.; Albrecht, L.; Boyd, R. J. Effect of Counterions on the Protonation State in a Poly(G)-Poly(C) Radical Cation. *J. Phys. Chem. B* **2011**, *115* (49), 14885–14890.
- (36) Cornell, W. D.; Cieplak, P.; Bayly, C. I.; Gould, I. R.; Merz, K. M.; Ferguson, D. M.; Spellmeyer, D. C.; Fox, T.; Caldwell, J. W.; Kollman, P. A. A Second Generation Force Field for the Simulation of Proteins, Nucleic Acids, and Organic Molecules. *J. Am. Chem. Soc.* **1995**, *117* (19), 5179–5197.
- (37) Swanson, J. M. J.; Adcock, S. A.; McCammon, J. A. Optimized Radii for Poisson-Boltzmann Calculations with the AMBER Force Field. *J. Chem. Theory Comput.* **2005**, *1* (3), 484–493.
- (38) Tuccinardi, T.; Martinelli, A.; Nuti, E.; Carelli, P.; Balzano, F.; Uccello-Barretta, G.; Murphy, G.; Rossello, A. Amber Force Field Implementation, Molecular Modelling Study, Synthesis and MMP-1/MMP-2 Inhibition Profile of (R)- and (S)-N-hydroxy-2-(N-isopropoxybiphenyl-4-ylsulfonamido)-3-methylbutanamides. *Bioorg. Med. Chem.* **2006**, *14* (12), 4260–4266.
- (39) Altun, A.; Yokoyama, S.; Morokuma, K. Spectral Tuning in Visual Pigments: An ONIOM(QM:MM) Study on Bovine Rhodopsin and its Mutants. *J. Phys. Chem. B* **2008**, *112* (22), 6814–6827.
- (40) Wang, J.; Wolf, R. M.; Caldwell, J. W.; Kollman, P. A.; Case, D. A. Development and Testing of a General Amber Force Field. *J. Comput. Chem.* **2004**, *25* (9), 1157–1174.
- (41) Lu, Y.; Shi, T.; Wang, Y.; Yang, H.; Yan, X.; Luo, X.; Jiang, H.; Zhu, W. Halogen Bonding—A Novel Interaction for Rational Drug Design? *J. Med. Chem.* **2009**, *52* (9), 2854–2862.
- (42) Bakowies, D.; Thiel, W. Hybrid Models for Combined Quantum Mechanical and Molecular Mechanical Approaches. *J. Phys. Chem.* **1996**, *100* (25), 10580–10594.
- (43) Singh, U. C.; Kollman, P. A. A Combined Ab Initio Quantum Mechanical and Molecular Mechanical Method for Carrying out Simulations on Complex Molecular Systems: Applications to the CH₃Cl + Cl[−] Exchange Reaction and Gas Phase Protonation of Polyethers. *J. Comput. Chem.* **1986**, *7* (6), 718–730.
- (44) Vreven, T.; Byun, K. S.; Komaromi, I.; Dapprich, S.; Montgomery, J. A.; Morokuma, K.; Frisch, M. J. Combining Quantum Mechanics Methods with Molecular Mechanics Methods in ONIOM. *J. Chem. Theory Comput.* **2006**, *2* (3), 815–826.
- (45) Guest, W. C.; Cashman, N. R.; Plotkin, S. S. A Theory for the Anisotropic and Inhomogeneous Dielectric Properties of Proteins. *Phys. Chem. Chem. Phys.* **2011**, *13* (13), 6286–6295.
- (46) Patargias, G. N.; Harris, S. A.; Harding, J. H. A Demonstration of the Inhomogeneity of the Local Dielectric Response of Proteins by Molecular Dynamics Simulations. *J. Chem. Phys.* **2010**, *132* (23), 235103.
- (47) Cheong, P. H.; Yun, H.; Danishefsky, S. J.; Houk, K. N. Torsional Steering Controls the Stereoselectivity of Epoxidation in the Guanacastepene A Synthesis. *Org. Lett.* **2006**, *8* (8), 1513–1516.

- (48) Vreven, T.; Mennucci, B.; da Silva, C. O.; Morokuma, K.; Tomasi, J. The ONIOM-PCM Method: Combining the Hybrid Molecular Orbital Method and the Polarizable Continuum Model for Solvation. Application to the Geometry and Properties of a Merocyanine in Solution. *J. Chem. Phys.* **2001**, *115* (1), 62–72.
- (49) Frisch, M. J.; Trucks, G. W.; Schlegel, H. B.; Scuseria, G. E.; Robb, M. A.; Cheeseman, J. R.; Scalmani, G.; Barone, V.; Mennucci, B.; Petersson, G. A.; et al. *Gaussian 09*; Gaussian, Inc.: Wallingford, CT, USA, 2009.
- (50) Law, V.; Knox, C.; Djoumbou, Y.; Jewison, T.; Guo, A. C.; Liu, Y.; Maciejewski, A.; Arndt, D.; Wilson, M.; Neveu, V.; et al. DrugBank 4.0: Shedding New Light on Drug Metabolism. *Nucleic Acids Res.* **2014**, *42* (D1), D1091–D1097.
- (51) Kim, C. U.; Chen, X.; Mendel, D. B. Neuraminidase Inhibitors as Anti-Influenza Virus Agents. *Antiviral Chem. Chemother.* **1999**, *10* (4), 141–154.
- (52) Varghese, J. N.; McKimm-Breschkin, J. L.; Caldwell, J. B.; Kortt, A. A.; Colman, P. M. The Structure of the Complex Between Influenza Virus Neuraminidase and Sialic Acid, the Viral Receptor. *Proteins: Struct., Funct., Genet.* **1992**, *14* (3), 327–332.
- (53) Hayden, F. G.; Osterhaus, A. D. M. E.; Treanor, J. J.; Fleming, D. M.; Aoki, F. Y.; Nicholson, K. G.; Bohnen, A. M.; Hirst, H. M.; Keene, O.; Wightman, K. Efficacy and Safety of the Neuraminidase Inhibitor Zanamivir in the Treatment of Influenzavirus Infections. *N. Engl. J. Med.* **1997**, *337* (13), 874–880.
- (54) Resetarits, D. E.; Bates, T. R. Errors in Chlorothiazide Bioavailability Estimates Based on a Bratton-Marshall Colorimetric Method for Chlorothiazide in Urine. *J. Pharm. Sci.* **1979**, *68* (1), 126–127.
- (55) Prichard, B. N.; Johnston, A. W.; Hill, I. D.; Rosenheim, M. L. Bethanidine Guanethidine and Methyldopa in Treatment of Hypertension: a within-Patient Comparison. *Br. Med. J.* **1968**, *1* (5585), 135–144.
- (56) Chawner, J. A.; Gilbert, P. A Comparative Study of the Bactericidal and Growth Inhibitory Activities of the Bisbiguanides Alexidine and Chlorhexidine. *J. Appl. Bacteriol.* **1989**, *66* (3), 243–252.
- (57) Albert, M.; Feiertag, P.; Hayn, G.; Saf, R.; Hönig, H. Structure–Activity Relationships of Oligoguanidines Influence of Counterion, Diamine, and Average Molecular Weight on Biocidal Activities. *Biomacromolecules* **2003**, *4* (6), 1811–1817.
- (58) Wexselblatt, E.; Esko, J. D.; Tor, Y. On Guanidinium and Cellular Uptake. *J. Org. Chem.* **2014**, *79* (15), 6766–6774.
- (59) Mehler, E. L.; Guarnieri, F. A Self-Consistent, Microenvironment Modulated Screened Coulomb Potential Approximation to Calculate pH-Dependent Electrostatic Effects in Proteins. *Biophys. J.* **1999**, *77* (1), 3–22.
- (60) Demchuk, E.; Wade, R. C. Improving the Continuum Dielectric Approach to Calculating pKas of Ionizable Groups in Proteins. *J. Phys. Chem.* **1996**, *100* (43), 17373–17387.
- (61) Nielsen, J. E.; Vriend, G. Optimizing the Hydrogen-Bond Network in Poisson–Boltzmann Equation-based pKa Calculations. *Proteins: Struct., Funct., Genet.* **2001**, *43* (4), 403–412.
- (62) Søndergaard, C. R.; Olsson, M. H. M.; Rostkowski, M.; Jensen, J. H. Improved Treatment of Ligands and Coupling Effects in Empirical Calculation and Rationalization of pKa Values. *J. Chem. Theory Comput.* **2011**, *7* (7), 2284–2295.
- (63) Dirr, L.; El-Deeb, I. M.; Guillon, P.; Carroux, C. J.; Chavas, L. M. G.; von Itzstein, M. The Catalytic Mechanism of Human Parainfluenza Virus Type 3 Haemagglutinin-Neuraminidase Revealed. *Angew. Chem., Int. Ed.* **2015**, *54* (10), 2936–2940.
- (64) Feig, M.; Karanicolas, J.; Brooks Iii, C. L. MMTSB Tool Set: Enhanced Sampling and Multiscale Modeling Methods for Applications in Structural Biology. *J. Mol. Graphics Modell.* **2004**, *22* (5), 377–395.
- (65) Pitera, J. W.; Falt, M.; van Gunsteren, W. F. Dielectric Properties of Proteins from Simulation: The Effects of Solvent, Ligands, pH, and Temperature. *Biophys. J.* **2001**, *80* (6), 2546–2555.
- (66) Espinosa, E.; Molins, E.; Lecomte, C. Hydrogen Bond Strengths Revealed by Topological Analyses of Experimentally Observed Electron Densities. *Chem. Phys. Lett.* **1998**, *285* (3–4), 170–173.
- (67) Quinonero, D.; Garau, C.; Frontera, A.; Ballester, P.; Costa, A.; Deya, P. M. Structure and Binding Energy of Anion- π and Cation- π Complexes: A Comparison of MP2, RI-MP2, DFT, and DF-DFT Methods. *J. Phys. Chem. A* **2005**, *109* (20), 4632–4637.